Journal of Power Sources 254 (2014) 338–344

Contents lists available at ScienceDirect

Journal of Power Sources

journal homepage: www.elsevier.com/locate/jpowsour

Evaluation of thermal stability in $Li_{0.2}Ni_xMn_{(1-x)/2}Co_{(1-x)/2}O_2$ ($x = 1/3$, 0.6, and 0.8) through X-ray absorption fine structure

Hiroaki Konishi*, Masanori Yoshikawa, Tatsumi Hirano, Kishio Hidaka

Hitachi Research Laboratory, Hitachi Ltd., 7-1-1 Ohmika-cho, Hitachi, Ibaraki 319-1292, Japan

HIGHLIGHTS

- Thermal stability of the charged cathode was influenced by the transition metal composition.
- Oxidation state and local structure of metal in the charged cathode changed at high temperature.
- The effects of Co and Mn substitution on the thermal stability were different.

ARTICLE INFO

Article history:
Received 14 June 2013
Received in revised form
8 December 2013
Accepted 27 December 2013
Available online 4 January 2014

Keywords:
Lithium ion secondary batteries
Cathode
Thermal stability
XAFS
Oxidation state
Local structure

ABSTRACT

High-Ni-content layer-structured cathode materials for lithium-ion secondary batteries have high capacity but they suffer from poor thermal stability. We studied the mechanism responsible for their thermal stability to make them more stable. We used X-ray absorption fine structure (XAFS) spectra to clarify the changes in the oxidation states and the local structures for each transition metal in $Li_{0.2}Ni_xMn_{(1-x)/2}Co_{(1-x)/2}O_2$ ($x = 1/3$, 0.6, and 0.8) at high temperature. The X-ray absorption near edge structure (XANES) spectra indicated that the oxidation state of Ni and Co changed due to heating. Although, pre-edge of XANES spectra indicated that the occupation sites of Co ions changed from octahedral to tetrahedral, Mn ions remained in the octahedral sites at high temperature. The extended X-ray absorption fine structure (EXAFS) results supported the change in the occupation sites of Co and Mn ions due to heating. It can be concluded that Co and Mn affected thermal stability of those Ni-based cathode materials differently. The Co ions migrated from octahedral to tetrahedral sites, and they stably occupy tetrahedral sites. Hence, so the structural change from spinel to rock-salt is suppressed. The oxidation state of Mn is stable and remains unchanged in layer structure at high temperature.

1. Introduction

Automotive applications of lithium-ion secondary batteries such as those in plug-in hybrid electric vehicles (PHEVs) and electric vehicles (EVs) have recently started to expand. These applications require much higher energy density than those in other conventional applications. Therefore, high-capacity cathode materials such as high-Ni-content layer-structured cathode materials are increasingly attracting attention [1–4]. However, their poor thermal stability has prevented them from being used in automotive applications [5–8]. The crystal structure of $Li_{1-a}NiO_2$ has been reported to change from layer to spinel and subsequently rock-salt as temperature increases in $Li_{1-a}NiO_2$ [9–13], and a similar transition occurs in $Li_{1-a}NiMO_2$ (M: transition metal) [14–26]. Furthermore, the structure change was accompanied by the change of the occupation sites for nickel ions [11–13].

We previously reported the relationship between change in the crystal structure and release of oxygen from cathodes [26]. In particular, we found that the crystal structure of $Li_{0.2}Ni_xMn_{(1-x)/2}Co_{(1-x)/2}O_2$ ($x = 1/3$, 0.6, and 0.8) changed from layer to spinel and subsequently to rock-salt at high temperature. Temperature at which the phase transition decreased as the Ni content was increased. Although Co and Mn substitution for Ni effectively improves the thermal stability of Ni-based layered cathode materials, the effects of Co and Mn have yet to be clarified in detail. In the current study, therefore, we focused on the oxidation state and the local structure for each transition metal when the crystal structure changed. X-ray absorption fine structure (XAFS) measurements were carried out to evaluate these changes, and the effects of Co and Mn substitution on the thermal stability of Ni-based layered cathode materials.

* Corresponding author. Tel.: +81 294 52 5111x6089; fax: +81 294 52 7636.
E-mail address: hiroaki.konishi.yj@hitachi.com (H. Konishi).

0378-7753/$ – see front matter © 2014 Elsevier B.V. All rights reserved.
http://dx.doi.org/10.1016/j.jpowsour.2013.12.107

2. Experimental

Three $LiNi_xMn_{(1-x)/2}Co_{(1-x)/2}O_2$ (x = 1/3, 0.6, and 0.8) samples were synthesized by using a solid state reaction. Stoichiometric amounts of LiOH, NiO, MnO_2, and Co_3O_4 with 3% excess of LiOH were thoroughly mixed and pressed into pellets. The pellets were precalcined in an oxygen atmosphere at 600 °C for 10 h and then ground and pressed into pellets again. They were calcined at 1000 °C in air for x = 1/3, at 900 °C in oxygen for x = 0.6, and at 850 °C in oxygen for x = 0.8. We also prepared $Li_{0.2}Ni_xMn_{(1-x)/2}Co_{(1-x)/2}O_2$ (x = 1/3, 0.6, and 0.8) by applying electrochemical delithiation to the corresponding cathodes of samples prepared as described above. The cathodes were formed on aluminum foil by blade-coating a slurry consisting of active material, carbon, polyvinylidene difluoride (PVDF) (85:10:5 wt.%), and N-methyl pyrrolidone (NMP) solvent. They were dried, pressed, and cut in turn. The delithiated electrodes were prepared using test cells assembled with one of the cathodes, an anode of lithium metal foil, a separator, and a 1 M $LiPF_6$ solution of carbonate solvent mixture in an argon glove box. The cells were charged to the prescribed composition ($Li_{0.2}Ni_xMn_{(1-x)/2}Co_{(1-x)/2}O_2$) at a rate of C/20. After being charged, the electrodes were washed with dimethyl carbonate (DMC) and dried. The charged electrode were heated at 150–400 °C in an argon atmosphere for 1 h to expose them to anomalous high temperatures that might occur under various unsafe conditions, and then cooled to room temperature. The lithium content before and after heating was analyzed using inductively-coupled plasma (ICP). Cathode electrodes before and after heating at 400 °C were dissolved in the aqua regalis, and their compositions analyzed. X-ray diffraction (XRD) measurements made with a Rigaku diffractometer with a graphite monochromator and Cu Kα radiation at 40 kV and 40 mA were used to identify the crystal structures of samples before and after they were heated. The diffraction angles were scanned from 10 to 70° using a step scan method with a 0.02° step and a counting time of 1.5 s per step. X-ray absorption fine structure (XAFS) measurements clarified the oxidation state and the local structure in each transition metal. The Ni, Co, and Mn K-edge XAFS spectra of the prepared samples were measured in transmission mode. The measurements were carried out at BL-9C, Photon Factory (PF), KEK, Japan using a Si(111) double-crystal monochromator. The oxidation state of each transition metal was mainly evaluated by using X-ray absorption near-edge structure (XANES). The XANES spectra of samples were compared with those of the reference samples such as transition metal oxide and lithium transition metal oxide. An extended X-ray absorption fine structure (EXAFS) was used to analyze the local structure around each transition metal. The background was subtracted using an extrapolated Victoreen-plus-constant type function and the EXAFS oscillation $\chi(k)$ was extracted using cubic spline baseline functions. The resulting $\chi(k)$ was weighted with k^3 (k: wave-vector) to compensate for the damping of oscillations with increasing k. The data were then Fourier Transformed [4,27,28].

3. Results and discussion

3.1. Crystal structure of $Li_{0.2}Ni_xMn_{(1-x)/2}Co_{(1-x)/2}O_2$ (x = 1/3, 0.6, and 0.8) at high temperature

Our aim was to precisely analyze the changes in the crystal structure of $Li_{0.2}Ni_xMn_{(1-x)/2}Co_{(1-x)/2}O_2$ (x = 1/3, 0.6, and 0.8) due to heating that we had presented in our previous study [26]. Fig. 1 shows the XRD patterns of $Li_{0.2}Ni_xMn_{(1-x)/2}Co_{(1-x)/2}O_2$ (x = 1/3, 0.6, and 0.8) at 25 °C and heated at 150–400 °C. For x = 1/3, layer structure was maintained from 25 to 250 °C. A new peak at 2θ = 31° appeared at 300 °C, and it remained until 400 °C. This peak indicates that the transition metal ions occupy tetrahedral sites in spinel structure [11–19]. Above 400 °C, the intensity of the peak at 2θ = 18° decreased, and the peaks at 2θ = 38, 44 and 64° shifted to a smaller angle. These results are symptomatic of a change to rock-salt structure [11–19]. This means that transition metal ions partly migrated from tetrahedral to octahedral sites in the lithium layer. However, some of the transition metal ions remained at tetrahedral sites even at 400 °C, because the peak at 2θ = 31° remained.

The XRD results for x = 0.6 were similar to those for x = 1/3, except at one point. The change of the peaks at 2θ = 18, 38, 44 and 64° was above 350 °C. For x = 0.8, a peak at 2θ = 31° appeared at temperature as low as 200 °C, but the peak intensity decreased above 300 °C. Moreover, the intensity of the peaks at 2θ = 18 and

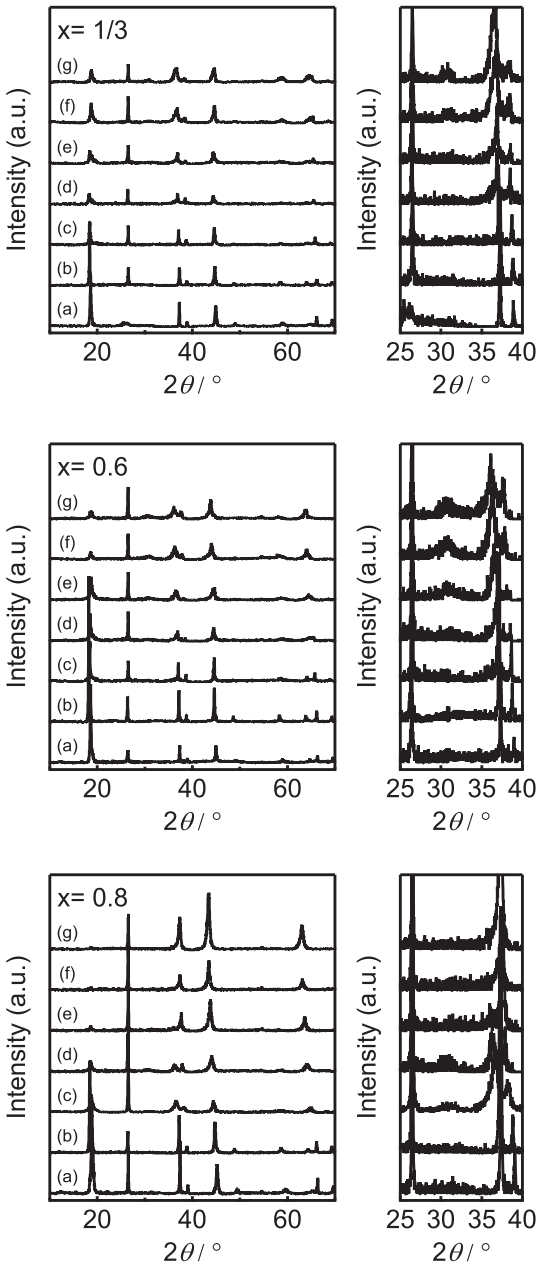

Fig. 1. XRD patterns of $Li_{0.2}Ni_xMn_{(1-x)/2}Co_{(1-x)/2}O_2$ (x = 1/3, 0.6, and 0.8) at 25 °C and heated at 150–400 °C: (a) 25 °C, (b) 150 °C, (c) 200 °C, (d) 250 °C, (e) 300 °C, (f) 350 °C, and (g) 400 °C.

Table 1
Lithium content of $Li_{0.2}Ni_xMn_{(1-x)/2}Co_{(1-x)/2}O_2$ ($x = 1/3$, 0.6, and 0.8) before and after heating at 400 °C.

x	Lithium content in $Li_{0.2}Ni_xMn_{(1-x)/2}Co_{(1-x)/2}O_2$	
	Before heating (25 °C)	After heating (400 °C)
1/3	0.21	0.21
0.6	0.22	0.22
0.8	0.22	0.22

37° decreased and those at 2θ = 38, 44, and 64° increased and shifted to a smaller angle. The peaks at 2θ = 18, 31, and 37° were barely observable at 400 °C. These results mean that for x = 0.8, transition metal ions migrated from octahedral sites in the transition metal layer to tetrahedral sites at lower temperature than those for x = 1/3 and 0.6. Furthermore, for x = 0.8, most of the transition metal ions migrated from tetrahedral to octahedral sites in the lithium layer.

We summarized that the XRD results above indicated (i) some of the transition metal ions migrated from octahedral to tetrahedral sites for $x = 1/3$ and 0.6; (ii) some of them migrated from octahedral sites in the transition metal layer to tetrahedral sites and then to octahedral sites in the lithium layer for $x = 0.8$; (iii) the temperature at which the crystal structure changes decreased as the Co and Mn content was decreased. However, details of the effects of Co and Mn were not be evaluated. Therefore, the changes in the oxidation state and the local structure for each transition metal due to heating were investigated.

It was reported that the crystal structure changes of the delithiated high-Ni-content cathodes were caused by reactions (1) and (2) detailed below [9,11–13].

$$Li_{0.2}MO_2(\text{Layer}) \rightarrow 0.4[Li_{0.5}M_{0.5}][M]_2O_4(\text{Spinel}) + 0.2O_2 \quad (1)$$

$$0.4[Li_{0.5}M_{0.5}][M]_2O_4(\text{Spinel}) \rightarrow [Li_{0.2}M]O_{1.2}(\text{Rock} - \text{salt}) + 0.2O_2 \quad (2)$$

Since the lithium might volatilize at high temperature, the lithium content before and after heating was measured using ICP analysis. Table 1 shows the lithium content in $Li_{0.2}Ni_xMn_{(1-x)/2}Co_{(1-x)/2}O_2$ (x = 1/3, 0.6, and 0.8) before and after heating at 400 °C, and it indicates that the lithium content barely changed. Therefore, the crystal structure change follows formula (1) and (2). Table 2 summarizes compositions, average oxidation numbers of transition metal calculated from the stoichiometric compositions, and occupation sites of transition metal for each crystal structure according to formula (1) and (2). However, the oxidation numbers and occupation sites in Table 2 are averages for Ni, Co, and Mn, all of which seem to be different. Therefore, we evaluated the differences by using XAFS measurements on each transition metal.

Table 2
Summary of compositions, average oxidation numbers of transition metal calculated from the stoichiometric compositions, and occupation sites of transition metal for each crystal structure.

Crystal structure	Composition	Average oxidation number	Occupation site for transition metal
Layer	$Li_{0.2}MO_2$	3.8	Octahedral site
Spinel	$Li_{0.2}MO_{1.6}$	3	Octahedral site, tetrahedral site
Rock-salt	$Li_{0.2}MO_{1.2}$	2.2	Octahedral site

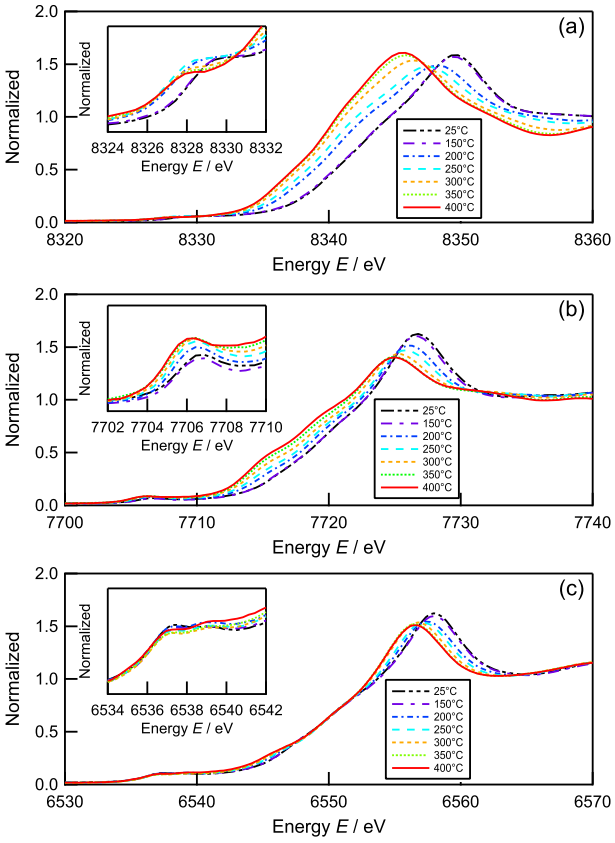

Fig. 2. (a) Ni, (b) Co, and (c) Mn K-edge XANES spectra of $Li_{0.2}Ni_{0.6}Mn_{0.2}Co_{0.2}O_2$ electrodes at 25 °C and heated at 150–400 °C.

3.2. Change in the oxidation state of $Li_{0.2}Ni_xMn_{(1-x)/2}Co_{(1-x)/2}O_2$ (x = 1/3, 0.6, and 0.8)

Fig. 2 shows the (a) Ni, (b) Co, and (c) Mn K-edge XANES spectra of $Li_{0.2}Ni_{0.6}Mn_{0.2}Co_{0.2}O_2$ electrodes at 25 °C and heated at 150–400 °C. The spectra each have a small pre-edge peak and a large peak. The pre-edge peak is associated with the dipole forbidden 1s→3d electronic transition. However, this transition is partly allowed by the hybridization of the 3d–4p orbital caused by the structural distortion around the central transition metal. The main peak is associated with the dipole allowed 1s→4p electronic transition [29–31]. The shift in the energy of the spectra and the intensity of the pre-edge are indicating the oxidation state and the local structure for the transition metal, respectively [4,27–33]. Fig. 2(a) and (b) shows that the XANES spectra of Ni and Co shifted to lower energies as the temperature increased. These shifts indicate a decrease in the oxidation number for transition metal. Fig. 2(c) shows that the absorption edge of the XANES spectra of Mn barely changed, and only the peak top energy shifted to the lower energy at high temperature. Therefore, the change in the oxidation state of Mn might be less than those of Ni and Co. Next, the influence of the transition metal composition on the XANES spectra was investigated. The half-height energy was used as an indicator of the energy shifts in the XANES spectra [4,27–33]. Fig. 3 summarizes the half-height energies from (a) Ni, (b) Co, and (c) Mn K-edge XANES spectra of $Li_{0.2}Ni_xMn_{(1-x)/2}Co_{(1-x)/2}O_2$ (x = 1/3, 0.6, and 0.8) electrodes at 25 °C and heated at 150–400 °C, together with the reference samples of transition metal oxide. Fig. 3(a) shows that the half-height energy of Ni decreased as the temperature increased. The

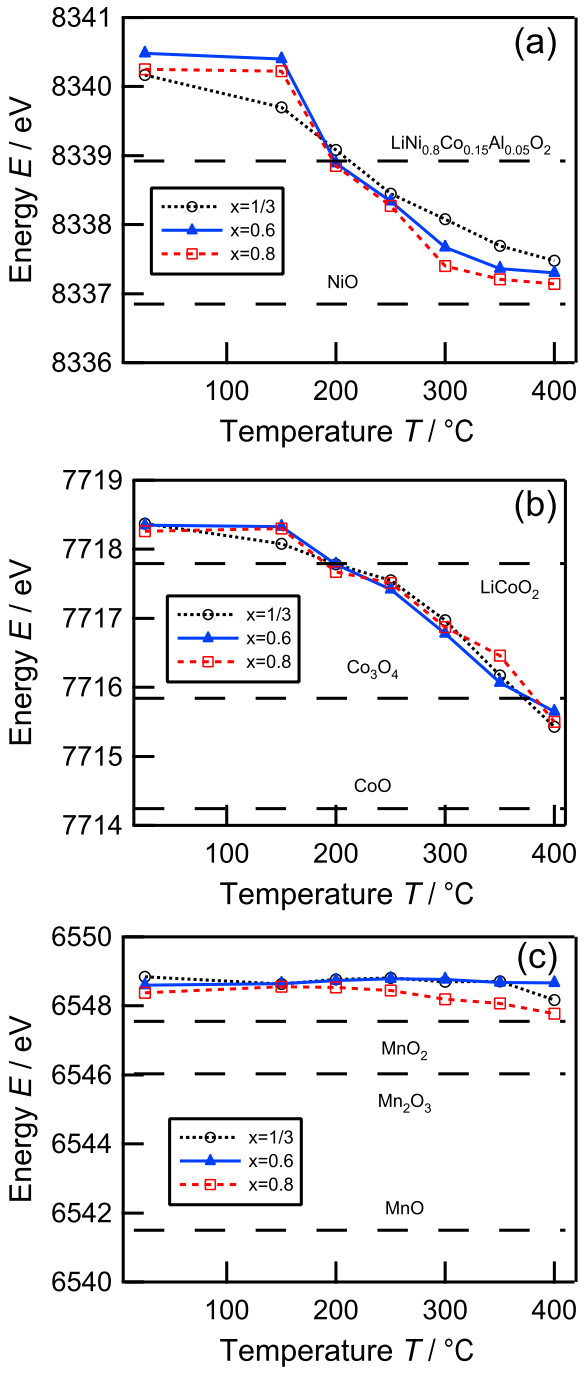

Fig. 3. Summary of the half-height energies from (a) Ni, (b) Co, and (c) Mn K-edge XANES spectra of $Li_{0.2}Ni_xMn_{(1-x)/2}Co_{(1-x)/2}O_2$ ($x = 1/3$, 0.6, and 0.8) electrodes at 25 °C and heated at 150–400 °C, together with the reference samples.

difference in the half-height energy of the all samples was small from 25 to 250 °C. On the other hand, the half-height energy of Ni at 300 °C decreased as the Ni content increased. This is the same tendency as the crystal structure change shown in Fig. 1. Fig. 3(b) shows that the half-height energy of Co decreased as the temperature increased regardless of the transition metal composition. Fig. 3(c) shows that the change of the half-height energy for Mn in all the samples from 25 to 400 °C was less than those of Ni and Co. This indicates that the stability of the high oxidation state for Mn was higher than those of Ni and Co. This might be contributed to that a high oxidation state, Mn^{4+}, is more stable than Mn^{3+} and Mn^{2+}.

Next, pre-edge spectra were evaluated. Pre-edge spectra of the XANES spectra are related to the distortion around the central transition metal in the octahedron and the occupation site of transition metal [29–31]. It has been reported that the intensity of the pre-edge peak is stronger when transition metal ions occupy tetrahedral sites than when they occupy octahedral sites [29–31]. The intensities of the pre-edge spectra of samples heated at 150–400 °C were compared with those of samples at 25 °C. Fig. 4 summarizes the pre-edge intensities of (a) Ni, (b) Co, and (c) Mn K-edge XANES spectra of $Li_{0.2}Ni_xMn_{(1-x)/2}Co_{(1-x)/2}O_2$ ($x = 1/3$, 0.6, and 0.8) electrodes at 25 °C and heated at 150–400 °C. Fig. 4(a) shows that the pre-edge intensities of Ni for all samples barely changed from 25 to 200 °C, but they decreased from 250 to 400 °C. Fig. 4(b) shows that the pre-edge intensities of Co for $x = 1/3$ and $x = 0.6$ increased above 300 and 200 °C, respectively. On the other hand, for $x = 0.8$, the pre-edge intensity of Co was strong from 200 to 250 °C, but it decreased above 300 °C. Fig. 4(c) shows that the pre-edge intensities of Mn for all spectra changed less than those of Co. The XRD results shown in Fig. 1 indicated that for $x = 1/3$ and 0.6, some of the transition metal ions occupied tetrahedral sites at high temperature. For $x = 0.8$, they migrated to tetrahedral sites below 200 °C and then to octahedral sites as the temperature increased. Since only the pre-edge intensity of Co increased as the temperature increased, Co ions might have migrated from octahedral to tetrahedral sites for all samples. In addition, they migrated from tetrahedral to octahedral sites in high Ni content materials.

On the other hand, pre-edge spectra shows that Ni and Mn ions did not occupy tetrahedral sites. However, since the crystal structure changed from layer to spinel and then to rock-salt in the high Ni content cathode, Ni ions migrated from octahedral sites in the transition metal layer to octahedral sites in the lithium layer [11–13].

Although, in going from the transition metal layer to the lithium layer, they might have gone through tetrahedral sites, because this pathway is energetically stable [30,34], it did not occupy these sites, since Ni ions at tetrahedral site is unstable [11,17]. Therefore, it could not have occupied tetrahedral sites. It can be concluded that they easily migrated to octahedral sites when the samples were heated.

We summarized that the results of the energy shift and pre-edge intensity from XANES spectra indicated (i) the oxidation states of Ni and Co were more changeable than that of Mn at high temperature. (ii) Nickel ions migrated from octahedral sites in the transition metal layer to octahedral sites in the lithium layer through tetrahedral sites. (iii) Cobalt ions migrated from octahedral to tetrahedral sites due to heating. In addition, they migrated from tetrahedral to octahedral sites in high Ni content materials. (iv) Manganese ions occupied octahedral sites at high temperature. Next, EXAFS analysis is applied to evaluate this mechanism.

3.3. Change in the local structure of $Li_{0.2}Ni_xMn_{(1-x)/2}Co_{(1-x)/2}O_2$ ($x = 1/3$, 0.6, and 0.8)

Fig. 5 shows the Fourier Transforms of (a) Ni, (b) Co, and (c) Mn K-edge EXAFS spectra of $Li_{0.2}Ni_{0.6}Mn_{0.2}Co_{0.2}O_2$ electrodes at 25 °C and heated at 150–400 °C. The first and second peaks at around 1.5 and 2.5 Å correspond to transition metal-oxygen and transition metal-transition metal interactions [4,27,28]. We focus on the oxidation state and the local structure for each transition metal in each crystal structure, so we analyzed the change in the first peak around 1.5 Å.

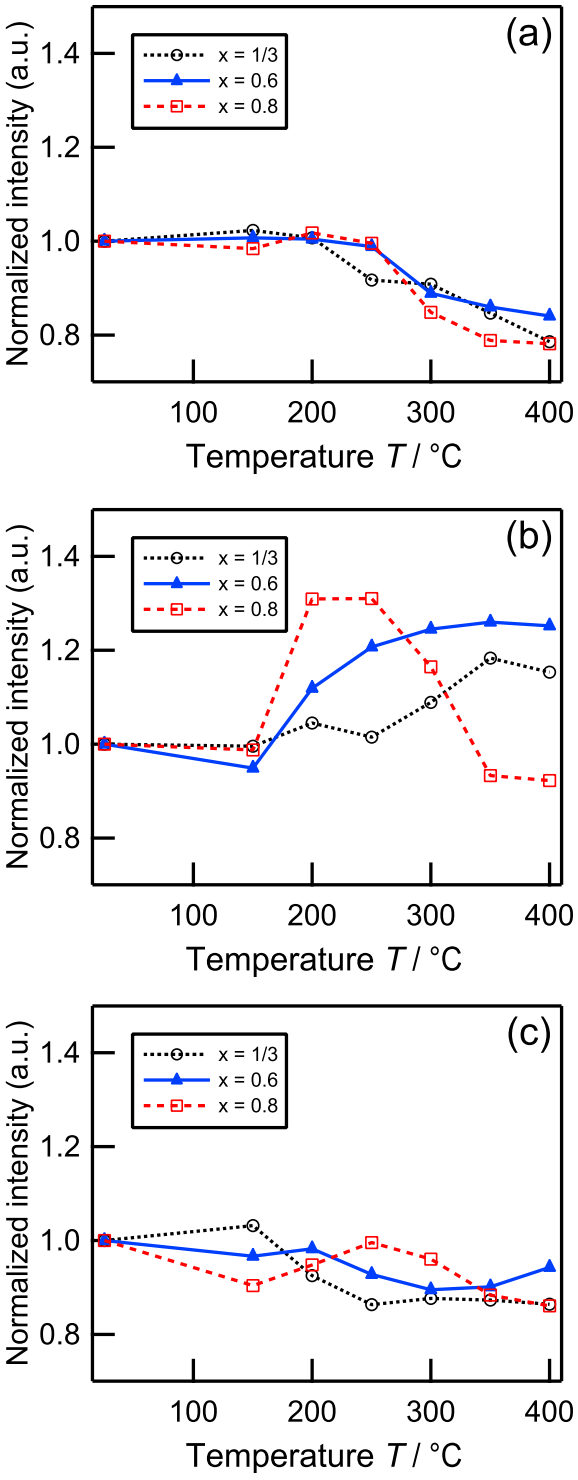

Fig. 4. Normalized pre-edge intensities of (a) Ni, (b) Co, and (c) Mn K-edge XANES spectra of $Li_{0.2}Ni_xMn_{(1-x)/2}Co_{(1-x)/2}O_2$ (x = 1/3, 0.6, and 0.8) electrodes at 25 °C and heated at 150–400 °C.

3.3.1. FT magnitude

The FT magnitude of M–O (M: metal) in all the transition metals changed due to heating. The decrease in the FT magnitude is related to an increase in the Debye–Waller factor and a decrease in the coordination number. The FT magnitude of Co–O and Mn–O decreased at high temperature. On the other hand, the FT magnitude of Ni–O decreased from 25 to 250 °C, but increased from 250 to 400 °C. The change in the FT magnitude of Co–O might be related to that of the Debye–Waller factor and the coordination number, since the occupation site of Co changed at high temperature. The occupation site of Mn did not change, so the change in the FT magnitude of Mn–O might be related to the Debye–Waller factor. The change in the FT magnitude of Ni–O was different from those of Co–O and Mn–O. The oxidation number of Ni at 25 °C is around 3.8^+ (Table 2). The XANES spectra indicated the oxidation number of Ni decreased as the temperature increased. When the oxidation state of Ni was 3^+, the Jahn–Teller effect caused there to be four short Ni–O distances and two long Ni–O distances, which decreased the FT magnitude of Ni–O [35–38]. As the oxidation state of Ni got closer to 2^+, the Jahn–Teller effect decreased, and so the FT magnitude probably increased.

3.3.2. Radial distance

Fig. 6 summarizes the radial distances of (a) Ni, (b) Co, and (c) Mn of $Li_{0.2}Ni_xMn_{(1-x)/2}Co_{(1-x)/2}O_2$ (x = 1/3, 0.6, and 0.8) electrodes at 25 °C and heated at 150–400 °C. Fig. 6(a) shows that the radial distance of Ni for all the samples increased as the temperature increased. The difference in the radial distance was small from 25 to 250 °C for all samples. On the other hand, the radial distance of Ni for $x = 0.8$ was larger than those of $x = 1/3$ and $x = 0.6$ at 300 °C. These were the same tendency as the result of the half-height energy in Fig. 3(a) shows the same tendency. This shows that the oxidation number of Ni decreased and radial distance of Ni increased at high temperature. The change for $x = 0.8$ is occurred at lower temperature than those for $x = 1/3$ and $x = 0.6$. Fig. 6(b)

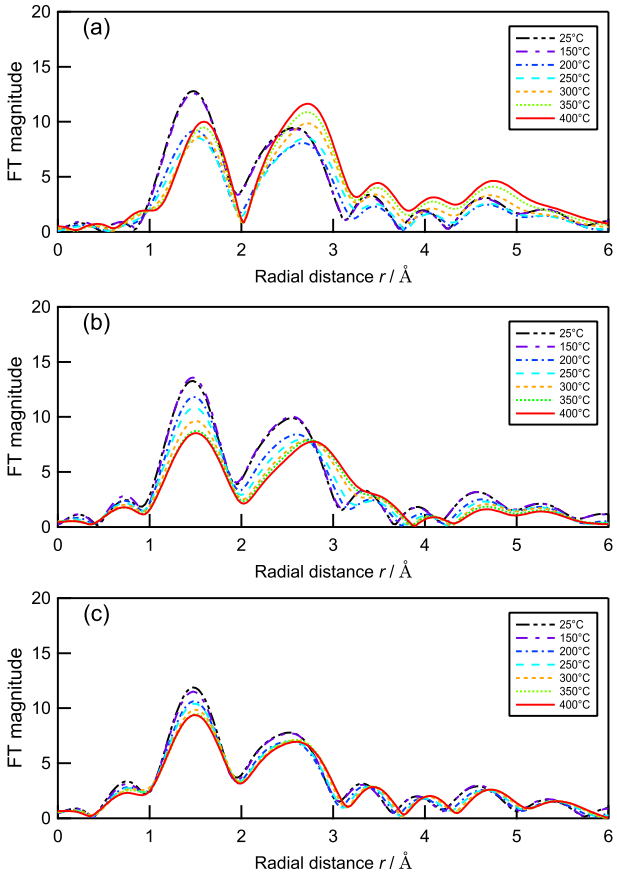

Fig. 5. Fourier Transforms of (a) Ni, (b) Co, and (c) Mn K-edge EXAFS spectra of $Li_{0.2}Ni_{0.6}Mn_{0.2}Co_{0.2}O_2$ electrodes at 25 °C and heated at 150–400 °C.

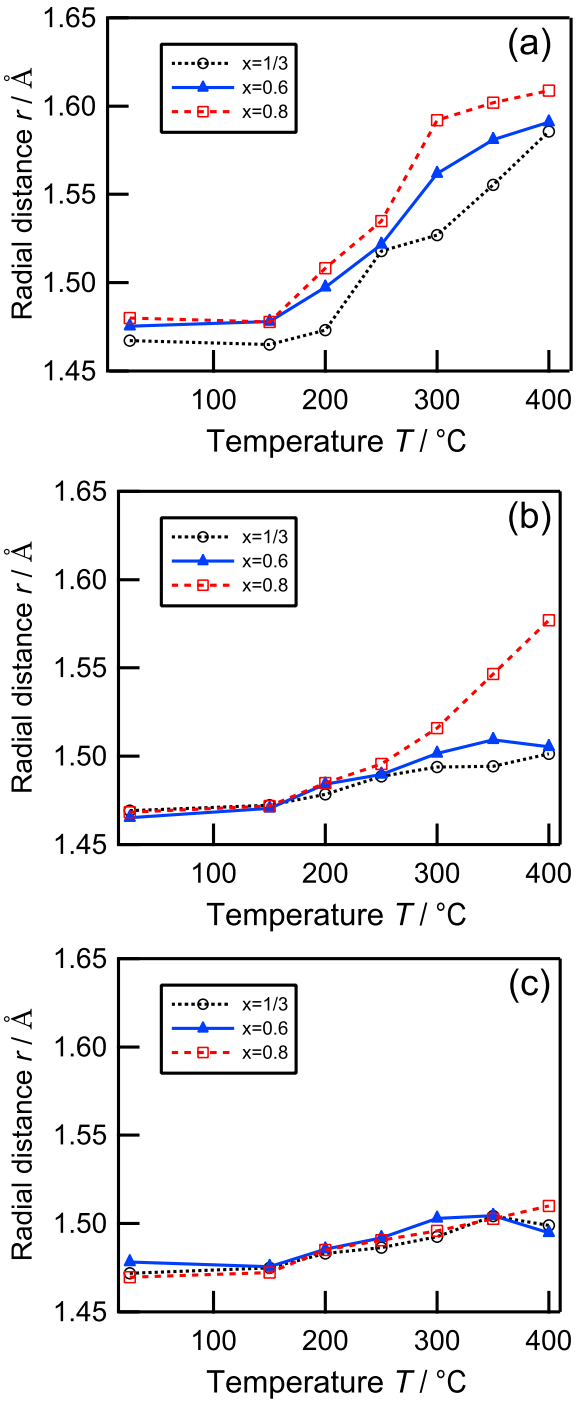

Fig. 6. Summary of the radial distances of (a)Ni, (b)Co, and (c)Mn of $Li_{0.2}Ni_xMn_{(1-x)/2}Co_{(1-x)/2}O_2$ ($x = 1/3$, 0.6, and 0.8) electrodes at 25 °C and heated at 150–400 °C.

shows that the radial distances of the samples were almost the same from 25 to 250 °C. However, the radial distance of Co for $x = 0.8$ became larger than those of $x = 1/3$ and $x = 0.6$ above 300 °C. The XRD and pre-edge intensity of Co K-edge XANES spectra of all the samples showed that Co ions migrated from octahedral to tetrahedral sites as a result of heating. Furthermore, only for $x = 0.8$, Co ions moved from tetrahedral to octahedral sites above 300 °C. Since the ionic radius of Co^{3+} at octahedral site (0.545 Å) is close to that of Co^{2+} at tetrahedral site (0.58 Å), radial distance of Co slightly changed despite the decrease in the oxidation number of Co for $x = 1/3$ and $x = 0.6$. On the other hand, for $x = 0.8$, the radial distance of Co substantially increased above 300 °C. This increase is related to the difference in the ionic radius of Co^{2+} at the tetrahedral site (0.58 Å) and at the octahedral site (0.65 Å) [39]. These results supported the change of the occupation sites for Co ions from octahedral to tetrahedral for $x = 1/3$ and $x = 0.6$, and from octahedral to tetrahedral then to octahedral for $x = 0.8$. Fig. 6(c) shows that the radial distance of Mn slightly changed due to heating. This result is the same tendency as the results of the half-height energy shown in Fig. 3(c). It can be concluded that the EXAFS analysis indicated (i) the radial distance of Ni increased because of increase in the ionic radius of all of the samples. (ii) The change in the radial distance of Co at high temperature varied with the transition metal composition. The changes for $x = 1/3$ and $x = 0.6$ were less than that for $x = 0.8$. This difference is related to that Co ions migrated from tetrahedral to octahedral sites only for $x = 0.8$. (iii) The change in the radial distance of Mn at high temperature was less than that of Ni. If the substituted content of Co and Mn was above 20%, Co ions occupied tetrahedral sites even at 400 °C. However, if the substitution content was 10%, Co ions migrated from tetrahedral to octahedral sites above 300 °C, and the crystal structure changed from spinel to rock-salt. The XAFS measurements evaluated the oxidation state and the local structure for each transition metal. The oxidation state and occupation site differed for each transition metal. It is known that Co and/or Mn substitution improves the thermal stability of Ni-based cathode materials. However, the effects of Co and Mn are different. Cobalt does not stabilize layer structure, and then the crystal structure changes from layer to spinel due to heating. However, Co ions can occupy tetrahedral sites, so they stabilize spinel structure and suppress the change to rock-salt structure. On the other hand, the oxidation state of Mn changed less than those of Ni and Co at high temperature. It stabilizes layer structure. Therefore, Mn is more effective for thermal stability than Co.

4. Conclusions

The effect of Co and Mn for the thermal stability in $Li_{0.2}Ni_xMn_{(1-x)/2}Co_{(1-x)/2}O_2$ ($x = 1/3$, 0.6, and 0.8) was investigated. XAFS measurements clarified that the change of the oxidation state and the occupation site for each transition metal. Since Co ions stably occupy tetrahedral sites, the crystal structure change from spinel to rock-salt was suppressed. However, this suppressive effect was small if the Co content was low (10%).

The oxidation state of Mn was stable, and the occupation site of Mn did not change at high temperature. Thus, Mn effectively prevented the crystal structure from layer to spinel. The results of this study show that elemental substitution improves the thermal stability of Ni-based cathode materials, but the effects differ for each element. Furthermore, the effect is also influenced by the content of Ni.

Acknowledgments

This work was supported by the New Energy and Industrial Technology Development Organization (NEDO) of Japan as part of the Li-EAD Project. We thank all those who participated in the project. We also thank Prof. T. Horiba of Mie University for the encouraging and helpful discussions he had with us on this paper.

This work was performed under the approval of the Photon Factory Program Advisory Committee (Proposal No. 2009I007, ;22-(2)-07, 23-(2)-09).

References

[1] J.R. Dahn, U. von Sacken, M.W. Juzkow, H. Al-Janaby, J. Electrochem. Soc. 138 (1991) 2207–2211.
[2] T. Ohzuku, A. Ueda, M. Nagayama, J. Electrochem. Soc. 148 (1993) 1862–1870.
[3] K.S. Lee, S.T. Myung, K. Amine, H. Yashiro, Y.K. Sun, J. Electrochem. Soc. 154 (2007) A971–A977.
[4] A. Deb, U. Bergmann, S.P. Cramer, E.J. Cairns, J. Electrochem. Soc. 154 (2007) A534–A541.
[5] J.R. Dahn, E.W. Fuller, M. Obrovac, U. Von Sacken, Solid State Ionics 69 (1994) 265–270.
[6] D.D. MacNeil, Z. Lu, Z. Chen, J.R. Dahn, J. Power Sources 108 (2002) 8–14.
[7] H. Arai, M. Tsuda, K. Saito, M. Hayashi, Y. Sakurai, J. Electrochem. Soc. 149 (2002) A401–A406.
[8] S. Jouanneau, D.D. MacNeil, Z. Lu, S.D. Beattie, G. Murphy, J.R. Dahn, J. Electrochem. Soc. 150 (2003) A1299–A1304.
[9] H. Arai, S. Okada, Y. Sakurai, J. Yamaki, Solid State Ionics 109 (1998) 295–302.
[10] H. Arai, Y. Sakurai, J. Power Sources 81–82 (1999) 401–405.
[11] M. Guilmard, L. Croguennec, D. Denux, C. Delmas, Chem. Mater. 15 (2003) 4476–4483.
[12] K.K. Lee, W.S. Yoon, K.B. Kim, K.Y. Lee, S.T. Hong, J. Power Sources 97–98 (2001) 321–325.
[13] K.K. Lee, W.S. Yoon, K.B. Kim, K.Y. Lee, S.T. Hong, J. Electrochem. Soc. 148 (2001) A716–A722.
[14] K.K. Lee, W.S. Yoon, K.B. Kim, J. Electrochem. Soc. 148 (2001) A1164–A1170.
[15] W.S. Yoon, M. Balasubramanian, X.Q. Yang, J. McBreen, J. Hanson, Electrochem. Solid State Lett. 8 (2005) A83–A86.
[16] W.S. Yoon, K.Y. Chung, M. Balasubramanian, J. Hanson, J. McBreen, X.-Q. Yang, J. Power Sources 163 (2006) 219–222.
[17] W.S. Yoon, J. Hanson, J. McBreen, X.Q. Yang, Electrochem. Commun. 8 (2006) 859–862.
[18] K.W. Nam, W.S. Yoon, X.Q. Yang, J. Power Sources 189 (2009) 515–518.
[19] M. Guilmard, L. Croguennec, C. Delmas, Chem. Mater. 15 (2003) 4484–4493.
[20] H. Bang, D.H. Kim, Y.C. Bae, J. Prakash, Y.K. Sun, J. Electrochem. Soc. 155 (2008) A952–A958.
[21] S.T. Myung, A. Ogata, K.S. Lee, S. Komaba, Y.K. Sun, H. Yashiro, J. Electrochem. Soc. 155 (2008) A374–A383.
[22] I. Belharouak, D. Vissers, K. Amine, J. Electrochem. Soc. 153 (2006) A2030–A2035.
[23] I. Belharouak, W. Lu, D. Vissers, K. Amine, Electrochem. Commun. 8 (2006) 329–335.
[24] I. Belharouak, W. Lu, J. Liu, D. Vissers, K. Amine, J. Power Sources 174 (2007) 905–909.
[25] N. Yabuuchi, Y.T. Kim, H.H. Li, Y. Shao-Horn, Chem. Mater. 20 (2008) 4936–4951.
[26] H. Konishi, T. Yuasa, M. Yoshikawa, J. Power Sources 196 (2011) 6884–6888.
[27] M. Balasubramanian, X. Sun, X.Q. Yang, J. McBreen, J. Electrochem. Soc. 147 (2000) 2903–2909.
[28] T. Nonaka, C. Okuda, Y. Seno, Y. Kondo, K. Koumoto, Y. Ukyo, J. Electrochem. Soc. 154 (2007) A353–A358.
[29] A. Deb, U. Bergmann, S.P. Cramer, E.J. Cairns, J. Appl. Phys. 97 (2005) 113523.
[30] S.M. Bak, K.W. Nam, W. Chang, X. Yu, E. Hu, S. Hwang, E.A. Stach, K.B. Kim, K.Y. Chung, X.Q. Yang, Chem. Mater. 25 (2013) 337–351.
[31] F. Farges, Phys. Rev. B 71 (2005) 155109.
[32] K.W. Nam, X.J. Wang, W.S. Yoon, H. Li, X. Huang, O. Haas, J. Bai, X.Q. Yang, Electrochem. Commun. 11 (2009) 913–916.
[33] W.E.Q. Grady, K.I. Pandya, K.E. Swider, D.A. Corrigan, J. Electrochem. Soc. 143 (1996) 1613–1616.
[34] S. Choi, A. Manthiram, J. Electrochem. Soc. 149 (2002) A1157–A1163.
[35] I. Nakai, K. Takahashi, Y. Shiraishi, T. Nakagome, F. Nishikawa, J. Solid State Chem. 140 (1998) 145–148.
[36] A. Rougier, C. Delmas, A.V. Chadwick, Solid State Commun. 94 (1995) 123–127.
[37] A.N. Mansour, J. McBreen, C.A. Melendres, J. Electrochem. Soc. 146 (1999) 2799–2809.
[38] A.N. Mansour, X.Q. Yang, X. Sun, J. McBreen, L. Croguennec, C. Delmas, J. Electrochem. Soc. 147 (2000) 2104–2109.
[39] R.D. Shannon, Acta Cryst. A 32 (1976) 751–767.